2013 IEEE/ASME International Conference on
Advanced Intelligent Mechatronics (AIM)
Wollongong, Australia, July 9-12, 2013

Model-based Fault Detection of Modular and Reconfigurable Robots with Joint Torque Sensing

Saleh Ahmad and Guangjun Liu, *Senior Member*, *IEEE*

Abstract— **In this paper, a Model-based approach to fault detection is proposed that is not reliant on measurement or estimation of joint acceleration. The proposed fault detection algorithm is intended for Modular and Reconfigurable Robots (MRR) with joint torque sensing. It functions by comparing the filtered joint torque command with a filtered torque estimate derived from the corresponding nonlinear dynamic model of MRR incorporating joint torque sensing. The proposed fault detection scheme is ideal for detecting faults in modular robots because of its independence on motion states of other modules for fault detection. Experiments were performed using three common faults associated with joint actuator and the results confirmed the theoretical proposal by successfully detecting faults independently for each joint module.**

I. INTRODUCTION

In many modern applications, robots have to operate in environments that could be unknown, hardly accessible, cost ineffective for men, or pose environmental dangers. Reliability and fault tolerance issues are at the heart of multitude of challenges posed at robots operating in remote and/or hazardous environments. It is therefore vital for robots to overcome the limitations enforced by failures through independent fault detection and fault-isolation, to permit an operator to continue utilizing the remaining functional capabilities.

Fault detection and fault tolerant control have been attracting a great deal of interest in the control engineering and robotics communities as it enables systems to continue operation, possibly at a reduced level, when some part of the system fails [1], [2], [3]. Effective fault detection and fault isolation form the backbone of active fault tolerant control schemes because it employs algorithms for providing early fault-related warnings, which in turn facilitates appropriate preventive actions to avoid complete system breakdown.

Several fault detection methods, [4], [5], [6], have been proposed in the existing literature for robot manipulators. In [4], a fault detection and isolation scheme designed on the bases of the inverse dynamics approach is presented for robot manipulators. In [5], joint torque measurement is used to estimate the power efficiency of MRR's joint. Residuals are generated by comparing the input and the output power of each MRR joint module. A fault detection scheme with online estimators to estimate the unknown constant sensor bias to diagnose sensor faults is investigated in [6]. The observer-based scheme proposed in [7] needs the measurement or estimation of accelerations and relies on residuals that are generated based on the comparison between predicted observer outputs with measured system outputs. A model-based fault detection approach that relies on residuals generated using filtered torque estimate is proposed in [8] and [9]. Online parameter estimation method for robotic systems is used in [10] to monitor and identify abrupt changes in system parameters due to faults. However, the dynamic model used in this work has been simplified by ignoring the coupling between joints which in turn necessitates the need for conservative thresholds to avoid false alarms.

In this paper, a model-based fault detection scheme is developed for MRR robots with joint torque sensing. The proposed scheme generates residuals for fault detection purposes by calculating the difference between filtered motor torque commands and filtered torque estimates. Since the torque commands and the torque estimates are filtered, the measurement or estimation of the robot joint accelerations are not required. The proposed scheme takes into account the uncertainties in system parameters, namely, the friction model parameters. The friction model parameters of each MRR joint are initially estimated using observer based techniques [11] and the resulting parameters are considered as nominal values. It is a well-known fact that these parameters change over time. Therefore, an adaptive law is used to update the friction model parameters online as a means of improving the sensitivity of the proposed fault detection scheme.

Three types of actuator faults are considered in this paper: *free-swinging* actuator fault, *ramp* actuator fault, and *saturated* actuator fault. The term *free-swinging* fault refers to a fault in a MRR joint module that causes the loss of actuator torque, like the loss of electrical power and brakes of an MRR joint or a mechanical failure in the drive system. The terms *ramp* actuator fault and the *saturated* actuator fault imply a joint that is gradually drifting from the actual torque command and suddenly saturated joint, respectively.

This paper is divided into five sections: Section II presents the dynamical model of MRR robots with joint torque sensing while the fault detection scheme is presented in Section III, experimental results in Section IV, and concluding remarks in Section V.

This work is supported in part by a grant from the Natural Sciences and Engineering Research Council (NSERC) of Canada and in part by the Canada Research Chair program.

S. Ahmad and G. Liu are with the Department of Aerospace Engineering, Ryerson University, 350 Victoria Street, Toronto, Ontario, Canada M5B 2K3. (G. Liu is the corresponding author. Phone: 416-979-5000; email: gjliu@ryerson.ca)

978-1-4673-5320-5/13/$31.00 ©2013 IEEE

II. Dynamic Model of Modular and Reconfigurable Robots

We consider modular and reconfigurable robots comprising of n modules, where each module is integrated with a rotary joint along with a speed reducer and a torque sensor as illustrated in Fig. 1.

The following notations are used in the dynamic model:
I_{mi} : rotor moment of inertia about the axis of rotation;
γ_i : reduction ratio of the speed reducer;
q_i : joint angle;
τ_{si} : coupling torque at the torque sensor location;
τ_i : output torque of the rotor;
z_{mi} : unit vector along the axis of rotation of the ith rotor;
z_i : unit vector along the axis of rotation of the ith joint; and
$F_i(\dot{q}_i, \tau_{si})$: joint friction which is assumed to be function of the joint velocity and the joint load. The dynamic model of

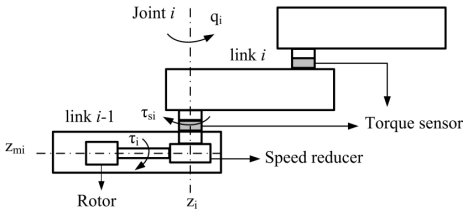

Fig. 1. Schematic diagram of one MRR joint module.

each joint of the MRR robot that was previously formulated in [12] is given by:
For the base module, $i = 1$,

$$I_{m1}\gamma_1\ddot{q}_1 + F_1(\dot{q}_1, \tau_{s1}) + \gamma_1^{-1}\tau_{s1} = \tau_1 \tag{1}$$

For the second module from the base, $i = 2$,

$$I_{m2}\gamma_2\ddot{q}_2 + F_2(\dot{q}_2, \tau_{s2}) + I_{m2}z_{m2}^T z_1 \ddot{q}_1 + \gamma_2^{-1}\tau_{s2} = \tau_2 \tag{2}$$

For $i \geq 3$,

$$\begin{aligned} &I_{mi}\gamma_i\ddot{q}_i + I_{mi}\sum_{j=1}^{i-1} z_{mi}^T z_j \ddot{q}_j + F_i(\dot{q}_i, \tau_{si}) \\ &+ I_{mi}\sum_{j=2}^{i-1}\sum_{k=1}^{j-1} z_{mi}^T(z_k \times z_j)\dot{q}_k\dot{q}_j + \gamma_i^{-1}\tau_{si} = \tau_i \end{aligned} \tag{3}$$

The joint friction, $f_i(\dot{q}_i, \tau_{si})$, is modeled to include the same frictional forces considered in [13]; however, to reflect the friction dependency on the payload, the friction is assumed to be function of the joint velocity and the payload that is measured by the intergraded joint torque sensor [14].

$$F_i(\dot{q}_i, \tau_{si}) = B_i\dot{q}_i + (g(\tau_{si})F_{ci} + F_{si}e^{-F_{\tau i}\dot{q}_i^2})sat(\dot{q}_i) \tag{4}$$

where B_i denotes the viscous friction coefficient, F_{ci} denotes the magnitude of the Coulomb friction related parameter at zero payload, F_{si} denotes the static friction related parameter, and $F_{\tau i}$ is a positive parameter related to the Stribeck effect. The saturation function is defined as

$$sat(\dot{q}_i) = \begin{cases} 1 & for\ \dot{q}_i > 0 \\ 0 & for\ \dot{q}_i = 0 \\ -1 & for\ \dot{q}_i < 0 \end{cases} \tag{5}$$

The function $g(\tau_{si})$ is defined as follows

$$g(\tau_{si}) \triangleq 1 + g_1 \mid \tau_{si} \mid + g_2 \mid \tau_{si} \mid^2 \tag{6}$$

where g_1 and g_2 are positive numbers used to emulate the payload-dependent Coulomb friction effect. The payload dependent friction is modeled as quadratic form to better preserve the problem nature [15]. In order to implement the proposed fault detection scheme that adaptively updates the joint friction parameters, it is first necessary to *linearize* the nonlinear friction model around the nominal values of the friction parameters similarly as in [13]

$$\begin{aligned} F_{si}e^{-F_{\tau i}\dot{q}_i^2} &\cong \hat{F}_{si}e^{-\hat{F}_{\tau i}\dot{q}_i^2} - \tilde{F}_{si}e^{-\hat{F}_{\tau i}\dot{q}_i^2} \\ &+ \hat{F}_{si}e^{-\hat{F}_{\tau i}\dot{q}_i^2}\dot{q}_i^2\tilde{F}_{\tau i} \end{aligned} \tag{7}$$

where $\hat{B}_i$, $\hat{F}_{ci}$, $\hat{F}_{si}$, $\hat{F}_{\tau i}$ denote the nominal values of their respective parameters and the parametric model uncertainty is defined as $\tilde{F}_i = \hat{F}_i - F_i$; therefore

$$\begin{aligned} F_{si}e^{-F_{\tau i}\dot{q}_i^2} &\cong F_{si}e^{-\hat{F}_{\tau i}\dot{q}_i^2} - F_{\tau i}\hat{F}_{si}\dot{q}_i^2 e^{-\hat{F}_{\tau i}\dot{q}_i^2} \\ &+ \hat{F}_{si}\hat{F}_{\tau i}\dot{q}_i^2 e^{-\hat{F}_{\tau i}\dot{q}_i^2} \end{aligned} \tag{8}$$

Substituting the "linearized" term $F_{si}e^{-F_{\tau i}\dot{q}_i^2}$ of (8) into the friction model (4) yields

$$\begin{aligned} F_i(\dot{q}_i, \tau_{si}) &= B_i\dot{q}_i + (g(\tau_{si})F_{ci} + F_{si}e^{-\hat{F}_{\tau i}\dot{q}_i^2} \\ &- F_{\tau i}\hat{F}_{si}\dot{q}_i^2 e^{-\hat{F}_{\tau i}\dot{q}_i^2})sat(\dot{q}_i) + \Phi_i sat(\dot{q}_i) \end{aligned} \tag{9}$$

where $\Phi_i = \hat{F}_{si}\hat{F}_{\tau i}\dot{q}_i^2 e^{-\hat{F}_{\tau i}\dot{q}_i^2}$. The friction model can be written in a compact form as

$$F_i(\dot{q}_i, \tau_{si}) = Y_i(\dot{q}_i, \tau_{si})\theta_i + \Phi_i sat(\dot{q}_i) \tag{10}$$

where $Y_i(\dot{q}_i, \tau_{si}) \in \Re^{1\times 4}$ denotes a known vector whose elements are functions of $\dot{q}_i$ and τ_{si}; $\theta_i \in \Re^4$ contains the uncertain friction parameters.

$$\begin{aligned} \theta_i &= [B_i \quad F_{ci} \quad F_{si} \quad F_{\tau i}]^T \\ Y_i(\dot{q}_i, \tau_{si}) &= \left[\dot{q}_i \quad g(\tau_{si})sat(\dot{q}_i) \quad \Psi \quad -\hat{F}_{si}\dot{q}_i^2\Psi\right] \end{aligned} \tag{11}$$

and $\Psi = e^{-\hat{F}_{\tau i}\dot{q}_i^2}sat(\dot{q}_i)$. The dynamical equation of the ith joint module can be rewritten as

$$\begin{aligned} &M_i\ddot{q}_i(t) + Y_i(\dot{q}_i(t), \tau_{si}(t))\theta_i + \Phi_i(\dot{q}_i(t))sat(\dot{q}_i(t)) \\ &+ \delta_i(t) + \gamma_i^{-1}\tau_{si}(t) = \tau_i(t) \end{aligned} \tag{12}$$

where, $M_i = I_{mi}\gamma_i$ and the term $\delta_i(t) \in \Re^1$ comprise of coupling effects between lower $i-1$ joints and the ith joint, given by

$$\delta_i(t) = \begin{cases} 0 & \text{for } i = 1 \\ I_{m2}z_{m2}^T z_1 \ddot{q}_1 & \text{for } i = 2 \\ I_{mi}\sum\limits_{j=2}^{i-1}\sum\limits_{k=1}^{j-1} z_{mi}^T(z_k \times z_j)\dot{q}_k\dot{q}_j & \\ +I_{mi}\sum\limits_{j=1}^{i-1} z_{mi}^T z_j \ddot{q}_j & \text{for } i \geq 3 \end{cases} \tag{13}$$

Note that the coupling term $\delta_i(t)$ comprises of only the ith joint motor dynamics as the links dynamics are captured by the integrated joint torque sensor. With consideration of

actuator faults, the dynamical equation (12) can be rewritten as

$$M_i\ddot{q}_i(t) + Y_i(\dot{q}_i(t), \tau_{si}(t))\theta_i + \Phi_i(\dot{q}_i(t))sat(\dot{q}_i(t)) + \delta_i(t) + \gamma_i^{-1}\tau_{si}(t) + u_{-1}(t - T_f)\zeta_i(t) = \tau_i(t) \quad (14)$$

where $\zeta_i(t) \in \Re^1$ represents a fault in the ith MRR joint module, $u_{-1}(t - T_f)$ represents a unit step function, T_f is the time instant when fault occurs. The following property of dynamic equation (14) and the succeeding assumption are worth noting as they are used in the development of fault detection scheme.

Property 1: The accelerations and velocities of the stabilized and fault free joint modules are bounded, hence, the following upper bound exist [2]

$$|\delta_i(t)| \leq \bar{\delta}_i \quad (15)$$

Assumption 1: A controller is designed which ensures that in the absence of a fault (i.e., $\forall t < T_f$) $q_i(t)$, $\dot{q}_i(t)$, $\tau_i(t) \in \mathcal{L}_\infty$ and that $\lim_{t\to\infty} q_i(t) \to q_{di}(t)$ where $q_{di}(t) \in \Re^1$ is the desired ith joint trajectory.

Note that based on the form of the dynamic model given in (14), if $q_i(t)$, $\dot{q}_i(t)$, $\tau_i(t) \in \mathcal{L}_\infty$ it is clear that $\ddot{q}_i(t) \in \mathcal{L}_\infty$.

In the presence of an actuator fault, the dynamic equation (14) can be rewritten as follows

$$\zeta_i(t) = \tau_i(t) - [M_i\ddot{q}_i(t) + N_i(t)] \quad \forall\, t \geq T_f \quad (16)$$

where

$$N_i(t) \triangleq Y_i(\dot{q}_i(t), \tau_{si}(t))\theta_i + \Phi_i(\dot{q}_i(t))sat(\dot{q}_i(t)) + \delta_i(t) + \gamma_i^{-1}\tau_{si}(t)$$

Remark 1: In order to detect actuator faults, the following equation could be utilized

$$\zeta_i(t) = \tau_i(t) - [M_i\ddot{q}_i(t) + N_i(t)] \quad (17)$$

However, the method in (17) is deemed impractical for fault detection as it requires acceleration measurements. In addition, for the ith joint, the motion states of all lower joint modules are required to construct the coupling effect term, which makes this approach unsuitable for modular robots. The objective of the present work is to design a fault detection scheme that does not require acceleration measurements or motion states of other joints.

III. Model-based Fault Detection

The proposed fault detection scheme is described in this section. The torque command of the ith joint module is filtered and compared with a filtered torque estimate that is derived from its dynamic equation given in (14). Driven by the desire of eliminating joint acceleration measurements from the fault detection scheme, a filtered torque signal denoted by, $\tau_{fi}(t) \in \Re^1$ is defined as follows

$$\tau_{fi}(t) = f(t) * \tau_i(t) \quad (18)$$

where the symbol $*$ denotes the standard convolution operation, and the low-pass filter function $f(t)$ is given by

$$f(t) = \alpha e^{-\beta t} \quad (19)$$

where α, $\beta \in \Re^1$ are positive filter constants.

Remark 2: As a result of the filtering, the filtered fault signal is delayed from the actual fault, although the delay can be mitigated by selecting large value of β.

Equation (14) can be rewritten in the following form

$$\tau_i = \dot{h}_i + \ell_i \quad (20)$$

where

$$\dot{h}_i = M_i\frac{d}{dt}\dot{q}_i(t)$$

$$\ell_i = Y_i(\dot{q}_i(t), \tau_{si}(t))\theta_i + \Phi_i(\dot{q}_i(t))sat(\dot{q}_i(t)) + \delta_i(t) + \gamma_i^{-1}\tau_{si}(t) + u_{-1}(t - T_f)\zeta_i(t)$$

Using the fact that convolution is distributive, substituting (20) into (18) yields

$$\tau_{fi}(t) = f(t) * \dot{h}_i + f(t) * \ell_i \quad (21)$$

Using standard convolution properties, one can write

$$f(t) * \dot{h}_i = \dot{f}(t) * h_i + f(0)h_i - f(t)h_i(0) \quad (22)$$

Substituting (22) and the expressions for h_i and ℓ_i into (21) yields

$$\tau_{fi}(t) = \dot{f}(t) * M_i\dot{q}_i(t) + f(0)M_i\dot{q}_i(t) + \zeta_{fi}(t) + \delta_{fi}(t) + Y_{fi}(q_i(t), \dot{q}_i(t), \tau_{si}(t))\theta_i - f(t)M_i\dot{q}_i(0) + f(t) * \{\gamma_i^{-1}\tau_{si}(t) + \Phi_i(\dot{q}_i(t))sat(\dot{q}_i(t))\} \quad (23)$$

where, $\delta_{fi} = f(t) * \delta_i$, θ_i is same constant parameter vector as defined in (10), $Y_{fi}(q_i(t), \dot{q}_i(t), \tau_{si}(t))$ denotes a measurable filtered regression vector and $\zeta_{fi}(t) \in \Re^1$ denotes the filtered fault signal defined as follows

$$\zeta_{fi}(t) = f(t) * u_{-1}(t - T_f)\zeta_i(t) \quad (24)$$

The following measurable prediction error (PE) is used to detect the fault at each joint module

$$e_i(t) = \tau_{fi}(t) - \hat{\tau}_{fi}(t) \quad (25)$$

where $\tau_{fi}(t)$ is defined in (23), and $\hat{\tau}_{fi}(t)$ is the filtered torque estimate to be derived.

It is clear from (23) that the only term that depends on motion states of other joint modules is $\delta_{fi}(t)$. This term represents the filtered coupling effect between the lower $i-1$ joints and the ith joint which is a function of the lower $i-1$ joints positions and velocities. For MRRs with joint torque sensing, the link dynamics are captured by the integrated torque sensors, and $\delta_{fi}(t)$ is coupling in the motor dynamics only as can be seen from (13). If each coupling term is considered as a modeling error then an adaptation law guaranteeing the convergence of filtered torque estimate to actual filtered torque in the existence of nonzero modeling errors can be designed. At this point, to explain the structure of the proposed fault detection scheme, the filtered coupling term $\delta_{fi}(t)$ is obtained using the known motion state of the lower $i-1$ joints. The filtered torque estimate is obtained by using the known nominal values of system parameters as follows

$$\hat{\tau}_{fi}(t) = \dot{f}(t) * M_i\dot{q}_i(t) + f(0)M_i\dot{q}_i(t) + \delta_{fi}(t) - f(t)M_i\dot{q}_i(0) + Y_{fi}(q_i(t), \dot{q}_i(t), \tau_{si}(t))\hat{\theta}_i + f(t) * \{\gamma_i^{-1}\tau_{si}(t) + \Phi_i(\dot{q}_i(t))sat(\dot{q}_i)(t)\} \quad (26)$$

Substituting (23) and (26) into (25) yields

$$e_i(t) = -Y_{fi}(q_i(t), \dot{q}_i(t), \tau_{si}(t))\tilde{\theta}_i + \zeta_{fi}(t) \tag{27}$$

where $\tilde{\theta}_i$ reflects the discrepancy between the actual and the nominal values of the MRR joint parameters and is given by

$$\tilde{\theta}_i = \hat{\theta}_i - \theta_i \tag{28}$$

An upper bound on the prediction error in equation (27) can be defined as follows

$$|e_i| \leq \rho_i(t) + |\zeta_{fi}(t)| \tag{29}$$

where $\rho_i(t) \in \Re^1$ is a positive bound that is selected to satisfy the following inequality

$$|Y_{fi}(q_i(t), \dot{q}_i(t), \tau_{si}(t))\tilde{\theta}_i| \leq \rho_i(t) \tag{30}$$

Therefore, a *dead-zone* residual function can be defined to indicate a fault as follows

$$D(e_i) = \begin{cases} 1 & if \quad |e_i| > \rho_i(t) \\ 0 & if \quad |e_i| \leq \rho_i(t) \end{cases} \tag{31}$$

For MRR robots, the fault detection of each joint module should not require the motion state of any other joint module. This is important due to the fact that joint modules may be added or removed at any time for MRR robots; therefore, it desirable to have a fault detection scheme that does not depend on the motion states of other joint modules. In order to craft a sensitive fault detection scheme that does not require the motion state of other joint modules, an online estimator for the uncertain parameters θ_i is designed while the coupling terms $\delta_i(t)$ are treated as modeling errors. In this case, the filtered torque estimate is designed as follows

$$\begin{aligned} \hat{\tau}_{fi}(t) &= \dot{f}(t) * M_i\dot{q}_i(t) + f(0)M_i\dot{q}_i(t) \\ &- f(t)M_i\dot{q}_i(0) + Y_{fi}(q_i(t), \dot{q}_i(t), \tau_{si}(t))\hat{\theta}_i \\ &+ f(t) * \{\gamma_i^{-1}\tau_{si}(t) + \Phi_i(\dot{q}_i(t))sat(\dot{q}_i(t))\} \end{aligned} \tag{32}$$

and the parameters' estimate is generated using prediction error driven gradient update law that is designed based on the switching σ-modification concepts [16], to avoid parameter drift due to the modeling error as follows

$$\dot{\hat{\theta}}_i(t) = \Gamma Y_{fi}^T e_i - \Gamma\sigma_s\hat{\theta}_i \tag{33}$$

where $\Gamma \in \Re^{4\times4}$ is adaptive gain with $\Gamma = \Gamma^T > 0$ and $\sigma_s \in \Re^1$ is given by

$$\sigma_s = \begin{cases} 0 & If \quad |\hat{\theta}_i(t)| < M_0 \\ \sigma_0(\frac{|\hat{\theta}_i(t)|}{M_0} - 1) & If \quad M_0 \leq |\hat{\theta}_i(t)| \leq 2M_0 \\ \sigma_0 & If \quad |\hat{\theta}_i(t)| \geq 2M_0 \end{cases} \tag{34}$$

where $M_0 > 0$, $\sigma_0 > 0$ are design constants and M_0 is chosen to be large enough so that $M_0 > |\theta_i|$. The prediction error in (25) becomes

$$e_i(t) = -Y_{fi}(q_i(t), \dot{q}_i(t), \tau_{si}(t))\tilde{\theta}_i + \delta_{fi}(t) + \zeta_{fi}(t) \tag{35}$$

A block diagram of the proposed fault detection scheme is shown in Fig. 2.

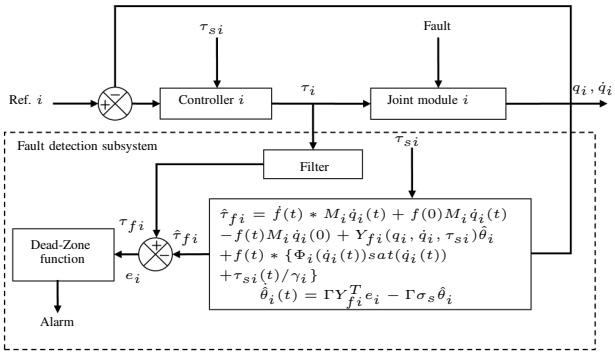

Fig. 2. Block diagram of fault detection of one MRR joint module.

In order to facilitate the subsequent analysis, we define the following non-negative Lyapunov-like function $V(\tilde{\theta}_i(t)) \in \Re$ as follows

$$V = \frac{\tilde{\theta}_i^T\Gamma^{-1}\tilde{\theta}_i}{2} \tag{36}$$

The time derivative of (36) yields the following equation

$$\dot{V} = \tilde{\theta}_i^T\Gamma^{-1}\dot{\tilde{\theta}}_i \tag{37}$$

Utilizing the fact that $\dot{\tilde{\theta}}_i(t) = \dot{\hat{\theta}}_i(t)$ and then substituting for (33), one obtains

$$\dot{V} = Y_{fi}\tilde{\theta}_i e_i - \sigma_s\tilde{\theta}_i^T\hat{\theta}_i \tag{38}$$

Substituting for $Y_{fi}\tilde{\theta}_i$ from (35) into (38) yields

$$\dot{V} = -e_i^2 + \delta_{fi}e_i - \sigma_s\tilde{\theta}_i^T\hat{\theta}_i + e_i\zeta_{fi} \tag{39}$$

In the absence of fault, $\zeta_{fi} = 0$, therefore

$$\dot{V} = -e_i^2 + \delta_{fi}e_i - \sigma_s\tilde{\theta}_i^T\hat{\theta}_i \leq -e_i^2 + |e_i|\bar{\delta}_{fi} - \sigma_s\tilde{\theta}_i^T\hat{\theta}_i \tag{40}$$

where $\bar{\delta}_{fi}$ is the upper bound for the coupling term δ_{fi}, i.e., $\bar{\delta}_{fi} = \sup_{t\geq0}\delta_{fi}$. Using completion of squares, one can write

$$-e_i^2 + |e_i|\bar{\delta}_{fi} \leq -\frac{e_i^2}{2} - \frac{1}{2}[e_i - \bar{\delta}_{fi}]^2 + \frac{\bar{\delta}_{fi}^2}{2} \leq -\frac{e_i^2}{2} + \frac{\bar{\delta}_{fi}^2}{2} \tag{41}$$

and

$$\begin{aligned} \sigma_s\tilde{\theta}_i^T\hat{\theta}_i &= \sigma_s(|\hat{\theta}_i|^2 - \theta_i^T\hat{\theta}_i) \\ &\geq \sigma_s|\hat{\theta}_i|(|\hat{\theta}_i| - M_0 + M_0 - |\theta_i|) \end{aligned} \tag{42}$$

Because $\sigma_s \geq 0$, $\sigma_s(|\hat{\theta}_i| - M_0) \geq 0$ and $M_0 > |\theta_i|$, it follows that

$$\begin{aligned} \sigma_s\tilde{\theta}_i^T\hat{\theta}_i &\geq \sigma_s|\hat{\theta}_i|(|\hat{\theta}_i| - M_0) + \sigma_s|\hat{\theta}_i|(M_0 - |\theta_i|) \\ &\geq \sigma_s|\hat{\theta}_i|(M_0 - |\theta_i|) \geq 0 \end{aligned} \tag{43}$$

From (43), it can be concluded that $-\sigma_s\tilde{\theta}_i^T\hat{\theta}_i \leq 0$ which mean that this term can only make $\dot{V}$ more negative. Because for $|\hat{\theta}_i| = |\tilde{\theta}_i + \theta_i| > 2M_0$, the term $-\sigma_s\tilde{\theta}_i^T\hat{\theta}_i = -\sigma_0\tilde{\theta}_i^T\hat{\theta}_i$. We also have

$$-\sigma_0\tilde{\theta}_i^T\hat{\theta}_i = -\sigma_0\tilde{\theta}_i^T(\tilde{\theta}_i + \theta_i) \leq -\sigma_0\frac{|\tilde{\theta}_i|^2}{2} + \sigma_0\frac{|\theta_i|^2}{2} \tag{44}$$

Therefore, from (41) and (44) one can rewrite (40) as

$$\dot{V} \leq -\frac{e_i^2}{2} - \sigma_0\frac{|\tilde{\theta}_i|^2}{2} + \frac{\bar{\delta}_{fi}^2}{2} + \sigma_0\frac{|\theta_i|^2}{2} \tag{45}$$

Adding and subtracting the term αV for some $\alpha > 0$, one obtains

$$\dot{V} \leq -\alpha V + \alpha(\frac{\tilde{\theta}_i^T \Gamma^{-1} \tilde{\theta}_i}{2}) - \frac{e_i^2}{2} - \sigma_0 \frac{|\tilde{\theta}_i|^2}{2} + \frac{\bar{\delta}_{fi}^2}{2} + \sigma_0 \frac{|\theta_i|^2}{2} \tag{46}$$

Because $\tilde{\theta}_i^T \Gamma^{-1} \tilde{\theta}_i \leq |\tilde{\theta}_i|^2 \lambda_{max}(\Gamma^{-1})$, equation (46) can be rewritten as

$$\dot{V} \leq -\alpha V + \alpha(\frac{|\tilde{\theta}_i|^2 \lambda_{max}(\Gamma^{-1})}{2}) - \frac{e_i^2}{2} - \sigma_0 \frac{|\tilde{\theta}_i|^2}{2} + \frac{\bar{\delta}_{fi}^2}{2} + \sigma_0 \frac{|\theta_i|^2}{2} \tag{47}$$

$$\dot{V} \leq -\alpha V - (\sigma_0 - \alpha \lambda_{max}(\Gamma^{-1})) \frac{|\tilde{\theta}_i|^2}{2} - \frac{e_i^2}{2} + \frac{\bar{\delta}_{fi}^2}{2} + \sigma_0 \frac{|\theta_i|^2}{2} \tag{48}$$

If we choose $0 < \alpha \leq \frac{\sigma_0}{\lambda_{max}(\Gamma^{-1})}$,

$$\dot{V} \leq -\alpha V + \frac{\bar{\delta}_{fi}^2}{2} + \sigma_0 \frac{|\theta_i|^2}{2} \tag{49}$$

Hence, for $V \geq V_0 = \frac{1}{2\alpha}(\bar{\delta}_{fi}^2 + \sigma_0 |\theta_i|^2)$, $\dot{V} \leq 0$, which implies that $V \in \mathcal{L}_\infty$ and therefore $\tilde{\theta}_i,\ \hat{\theta}_i \in \mathcal{L}_\infty$. Furthermore, according to (18) and *Assumption 1*, $Y_{fi},\ \dot{Y}_{fi},\ \tau_{fi},\ \dot{\tau}_{fi} \in \mathcal{L}_\infty$. Based on the fact that $Y_{fi},\ \tilde{\theta}_i \in \mathcal{L}_\infty$, one can utilize (35) to conclude that $e_i \in \mathcal{L}_\infty$. Since $Y_{fi},\ e_i \in \mathcal{L}_\infty$ it can be concluded from (33) that $\dot{\hat{\theta}}_i \in \mathcal{L}_\infty$. We can also use $-\sigma_0 \tilde{\theta}_i^T \hat{\theta}_i \leq -\sigma_0 \frac{|\hat{\theta}_i|^2}{2} + \sigma_0 \frac{|\theta_i|^2}{2}$ and rewrite (40) as

$$\dot{V} \leq -\frac{e_i^2}{2} + \frac{\bar{\delta}_{fi}}{2} - \sigma_0 \frac{|\hat{\theta}_i|^2}{2} + \sigma_0 \frac{|\theta_i|^2}{2} \tag{50}$$

Integrating both sides of (50) yields

$$\int_t^{t+T} (e_i^2 + \sigma_0 |\hat{\theta}_i|^2) d\tau \leq \int_t^{t+T} (\bar{\delta}_{fi} + \sigma_0 |\theta_i|^2) d\tau + 2[V(t) - V(t+T)] \leq c_0(\bar{\delta}_{fi} + \sigma_0) + c_1 \tag{51}$$

$\forall t \geq 0$ and $T > 0$ where $c_0 = max[1, |\theta_i|^2]$, $c_1 = 2 \sup_t [V(t) - V(t+T)]$, which implies that $e_i, \sqrt{\sigma_0}\hat{\theta} \in \mathcal{S}(\bar{\delta}_{fi} + \sigma_0)$. In addition, from equation (33), it follows that

$$\dot{\hat{\theta}}_i \in \mathcal{S}(\bar{\delta}_{fi} + \sigma_0) \tag{52}$$

Furthermore, when the coupling term $\delta_{fi} = 0$, because $-\sigma_s \tilde{\theta}_i^T \hat{\theta}_i \leq 0$ equation (40) implies that $e_i \in \mathcal{L}_2$. Based on the facts that $Y_{fi},\ \dot{Y}_{fi},\ e_i,\ \dot{\hat{\theta}}_i \in \mathcal{L}_\infty$, it can be concluded that $\dot{e}_i \in \mathcal{L}_\infty$. Therefore, since $e_i,\ \dot{e}_i \in \mathcal{L}_\infty$ and $e_i \in \mathcal{L}_2$, Barbălate's Lemma can be utilized to conclude that $\lim_{t\to\infty} |e_i| = 0$ in the absence of fault. Therefore, the boundedness of the prediction error e_i is proved.

Due to the fact that the residual given in (31) is based on fixed conservative threshold, we are motivated to design a new *dead-zone* update rule to modify the *dead-zone* threshold as $|e_i|$ decreases. The prediction error converge to a small value as the filtered torque estimate $\hat{\tau}_{fi}$ converge to a value close to the filtered torque τ_{fi}. The upper bound of the prediction error, ϱc_i, and the convergence time, t_{ci}, are determine experimentally for each joint module in absence of fault. Once ϱc_i and tc_i are known, the following *dead-zone* residual function is defined to indicate a fault.

$$D(e_i) = \begin{cases} 1 & if \quad |e_i| > \varrho_i(t) \\ 0 & if \quad |e_i| \leq \varrho_i(t) \end{cases} \tag{53}$$

where $\varrho_i(t)$ is selected as follows

$$\begin{array}{ll} \text{if} & (t \leq tc_i) \quad \text{then} \quad \varrho_i(t) = |e_i| + \epsilon \\ \text{else} & \varrho_i(t) = \varrho c_i \end{array}$$

and ϵ is a small positive constant.

Fig. 3. Two-link MRR robot.

IV. Experimental Results

The proposed fault detection scheme was implemented on a two-degrees-of-freedom, revolute MRR robot Fig. 3 the dynamics of which are described by Equations (1) and (2). The dynamic model's parameters, measured in SI units in the joint space, are listed in Table I. While the friction model parameters were determined experimentally, the rotor inertia and harmonic drive's reduction ratio of each joint were obtained from manufacturer's specification sheet. Distributed control method based on joint torque sensing [17] is used to ensure desired position tracking of each joint with a reasonable performance. For the experimental verification of the fault detection scheme, the friction parameters are assumed to be unknown or have changed over time due to lubricating and/or aging condition. The initial estimate of friction parameters, $\hat{\theta}_i(0)$, were selected to be $\pm 30\%$ of their actual values. The parameters estimate, $\hat{\theta}_i(t)$, of equation (32) was generated online based on (33). The gains and parameters of the adaptive update law in (33) were selected as follows: $\sigma_0 = 0.1, \Gamma = Diag\{3.5, 2, 2.25, 3\}, M_0$ was selected based on the experimentally determined values

TABLE I

Physical parameters of the two-link MRR robot

Parameter	Joint 1	Joint 2
Rotor inertia (kg-m2)	0.0000168	0.0000168
Gear ratio	101	101
Viscous friction coefficient (Nms/rad)	0.12	0.1
Static friction parameter (Nm)	0.0152	0.0143
Coulomb friction parameter (Nm)	0.015	0.0124
Stribeck effect parameter (Nm)	100	90
g_1	4.9	5.2
g_2	0.6	0.8

of the friction parameters θ_i, and the filter parameters are $\beta = 10$ and $\alpha = 1$ for both joints. A *free-swinging* actuator fault, a *ramp* actuator fault with $\vartheta_i = 1$, and a *saturation* actuator fault were injected into the two-link MRR system at $t = 29s$ for joint 1 and joint 2 in the first and second experiment, respectively. The results of these experiments are shown in Figs. 4–6 for joint 1 and Figs. 7–9 for joint 2. The left column of plots in Figs. 4–9 depicts the filtered torques and filtered torque estimates, the middle column depicts the prediction error in full time scale, and the right column of plots depicts the last $1.5s$ of experimental runtime to highlight when the fault is detected.

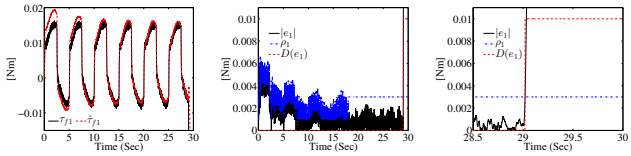

(a) Filtered torques (b) Prediction error (c) PE (zoom-in)

Fig. 4. Free-swinging actuator fault, joint 1.

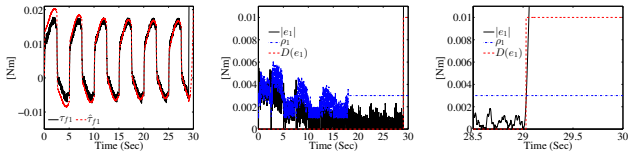

(a) Filtered torques (b) Prediction error (c) PE (zoom-in)

Fig. 5. Ramp actuator fault, joint 1.

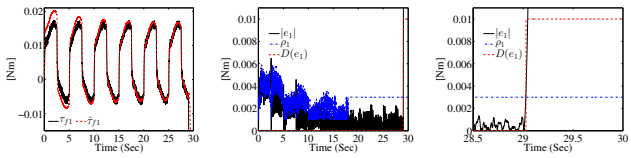

(a) Filtered torques (b) Prediction error (c) PE (zoom-in)

Fig. 6. Saturated actuator fault, joint 1.

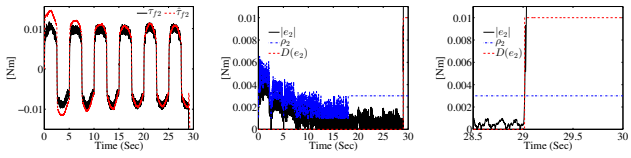

(a) Filtered torques (b) Prediction error (c) PE (zoom-in)

Fig. 7. Free-swinging actuator fault, joint 2.

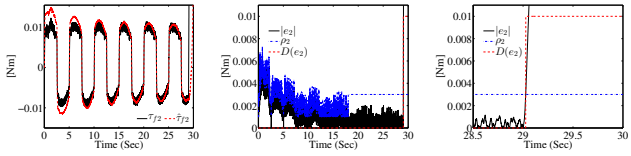

(a) Filtered torques (b) Prediction error (c) PE (zoom-in)

Fig. 8. Ramp actuator fault, joint 2.

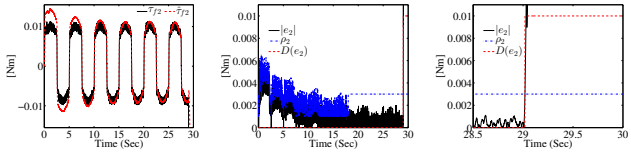

(a) Filtered torques (b) Prediction error (c) PE (zoom-in)

Fig. 9. Saturated actuator fault, joint 2.

V. CONCLUSIONS

In this paper a model-based fault detection scheme that does not require motion states of any other modules is proposed for MRR robots with joint torque sensing. Unlike some previously proposed fault detection schemes, measurements or estimations of joint accelerations are not required. Furthermore, as precise knowledge of the robot model and parameters may not be possible, the proposed fault detection scheme is designed to be robust to uncertainties in the system parameters. Experimental results have shown the efficiency of proposed fault detection scheme.

REFERENCES

[1] G. Liu, "Control of robot manipulators with consideration of actuator performance degradation and failures," in *Proc. IEEE Int. Conf. on Robot. and Autom.*, Seoul, Korea, May 2001, pp. 2566–2571.

[2] S. Abdul and G. Liu, "Decentralised fault tolerance and fault detection of modular and reconfigurable robots with joint torque sensing," in *Proc. IEEE Int. Conf. on Robot. and Autom.*, Pasadena, CA, USA, May 2008, pp. 3520–3526.

[3] G. Paviglianiti, F. Pierri, F. Caccavale, and M. Mattei, "Robust fault detection and isolation for proprioceptive sensors of robot manipulators," *Mechatronics*, vol. 20, no. 1, pp. 162–170, Feb. 2010.

[4] D. Brambilla, L. M. Capisani, A. Ferrara, and P. Pisu, "Fault detection for robot manipulators via second-order sliding modes," *IEEE Trans. on Ind. Electron.*, vol. 55, no. 11, pp. 3954–3963, Nov. 2008.

[5] J. Yuan, G. Liu, and B. Wu, "Power efficiency estimation-based health monitoring and fault detection of modular and reconfigurable robot," *IEEE Trans. on Ind. Electron.*, vol. 58, no. 10, pp. 4880–4887, Oct. 2011.

[6] X. Zhang, "Sensor bias fault detection and isolation in a class of nonlinear uncertain systems using adaptive estimation," *IEEE Trans. on Automat. Contr.*, vol. 56, no. 5, pp. 1220–1226, May 2011.

[7] F. Caccavale and I. D. Walker, "Observer-based fault detection for robot manipulators," in *Proc. IEEE Int. Conf. on Robot. and Autom.*, Albuquerque, NM, USA, Apr. 1997, pp. 2881–2887.

[8] W. E. Dixon, I. D. Walker, D. M. Dawson, and J. P. Hartranft, "Fault detection for robot manipulators with parametric uncertainty: a prediction error based approach," *IEEE Trans. on Robot. and Autom.*, vol. 16, no. 6, pp. 689–699, Dec. 2000.

[9] M. L. McIntyre, W. E. Dixon, D. M. Dawson, and I. D. Walker, "Fault identification for robot manipulators," *IEEE Trans. on Robot.*, vol. 21, no. 5, pp. 1028–1034, Oct. 2005.

[10] B. Freyermuth, "An approach to model-based fault diagnosis of industrial robots," in *Proc. IEEE Int. Conf. on Robot. and Autom.*, Sacramento, CA, USA, Apr. 1991, pp. 1350–1356.

[11] L. L. Tien, A. Albu-Schaffer, A. D. Luca, and G. Hirzinger, "Friction observer and compensation for control of robots with joint torque measurement," in *Proc. IEEE/RSJ Int. Conf. on Intel. Robot. and Sys.*, Nice, France, Sep. 2008, pp. 3789–3795.

[12] G. Liu, S. Abdul, and A. A. Goldenberg, "Stabilizing modular and reconfigurable robot joint by joint using torque sensing," *Robotica*, vol. 26, no. 1, pp. 75–84, Jan. 2008.

[13] G. Liu, A. A. Goldenberg, and Y. Zhang, "Precise slow motion control of a direct-drive robot arm with velocity estimation and friction compensation," *Mechatronics*, vol. 14, no. 7, pp. 821–834, Apr. 2004.

[14] P. Hamon, M. Gautier, and P. Garrec, "Dynamic identification of robots with a dry friction model depending on load and velocity," in *Proc. IEEE/RSJ Int. Conf. on Intell. Robot. and Syst.*, Taipei, Taiwan, Oct. 2010, pp. 6187–6193.

[15] W.-H. Zhu, E. Dupuis, and M. Doyon, "Adaptive control of harmonic drives," *ASME Trans. on Dyn. Syst., Measur., and Contr.*, vol. 129, no. 2, pp. 182–193, Aug. 2007.

[16] P. A. Ioannou and K. S. Tsakalis, "A robust direct adaptive controller," *IEEE Trans. on Automat. Contr.*, vol. 31, no. 11, pp. 1033–1043, Nov. 1986.

[17] S. Ahmad, H. Zhang, and G. Liu, "Multiple working mode control of door-opening with a mobile modular and reconfigurable robot," *IEEE/ASME Trans. on Mech.*, vol. 14, no. 99, pp. 1–12, Feb. 2012.